Experimental Investigation of Unreinforced Brick Masonry Walls in Flexure

Michael Craig Griffith[1]; Nelson T. K. Lam[2]; John Leonard Wilson[3]; and Kevin Doherty[4]

Abstract: This paper presents the results of static and dynamic tests on unreinforced brick masonry wall panels subject to out-of-plane loading. Fourteen wall panels were tested. The test program included static, free-vibration, and dynamic tests using harmonic support, impulse support, and earthquake support motion. The experimental results indicate that displacement, rather than inertia force amplitude, determines whether an unreinforced masonry wall will collapse during inertial (seismic) loading. An empirical force–displacement relationship is proposed that can be used for a substitute structure in a displacement-based method of analysis.

DOI: 10.1061/(ASCE)0733-9445(2004)130:3(423)

CE Database subject headings: Masonry; Earthquake loads; Flexure; Displacement; Walls; Panels.

Introduction

In recent years displacement-based (DB) design philosophies have gained popularity in the research arena for the seismic design and evaluation of ductile structures (e.g., Calvi and Kingsley 1995; Moehle 1996; Priestley 1997). However, designers have traditionally perceived unreinforced masonry (URM) as a brittle form of construction. It has been considered sensitive to peak ground accelerations so that DB philosophies have not been thought applicable. In contrast, a growing body of research has shown that dynamically loaded URM walls can often sustain accelerations well exceeding their ''quasistatic'' capabilities (Ewing and Kariotis 1981; Bariola et al. 1990; Lam et al. 1995). This dynamic ''reserve capacity'' to rock arises because in most cases the dynamic response is largely governed by stability mechanisms with geometric instability of a URM wall only occurring when the midheight displacement exceeds a stability limit (La Mendola et al. 1995). Indeed, research into face loaded infill masonry panels has shown that under dynamic loading one of the key responses governing wall stability is the size of the maximum displacement (Abrams et al. 1996). This suggests that DB philosophies could be used to provide a rational means of determining seismic design action for URM walls in preference to the traditional quasistatic force-based approach. Work along these lines is already well developed for the prediction of in-plane rocking capacity of URM walls (Magenes and Calvi 1997).

No static and few dynamic predictive models are able to account for the large displacement postcracking behavior and reserve capacity of URM walls when subjected to the transient characteristics of real earthquake excitations. Traditional quasistatic approaches are restricted to considerations taken at a critical snapshot during the response and, hence, the actual time-dependent characteristics are not modeled. As a result the reserve capacity to rock is not recognized, thus providing a conservative prediction of dynamic lateral capacity. While such conservative analysis procedures may be suitable for new structures, they may not be appropriate for the review of existing URM where an unacceptable economic penalty could be imposed should this reserve capacity not be considered. In recognition of this shortfall, a velocity-based approach founded on the equal-energy ''observation'' was developed (Priestly 1985), which considers the energy balance of the responding wall. The main disadvantage of this procedure is that the energy demand is very sensitive to the selection of elastic natural frequency and is only relevant for a narrow band of frequencies. Due to the above shortfalls, there is a need for the development of a rational, but simple, analysis procedure, encompassing the essence of the dynamic behavior and a wall's reserve capacity to rock.

The objective of this paper is to (1) summarize results from recent experimental investigations into the flexural behavior of URM walls and (2) to provide experimental evidence to support the proposed displacement-based design (DBD) model, which was introduced recently by Doherty et al. (2002). The development of the DBD method was based on parametric studies that employed a large volume of time-history analysis (THA) data. Information related to input into the THA would require validation, particularly in regard to the force–displacement and damping characteristics of URM walls. This is addressed in this paper. In addition, shaking table simulations of real earthquakes are used to demonstrate important trends related to the overall response behavior of URM walls. For example, the wall ultimate behavior is shown to be controlled significantly by displacement when the excitation possesses high frequency. This paper is intended to be of benefit to both engineering practitioners and researchers in terms of developing a better understanding of the factors that

[1]Associate Professor, Dept. of Civil and Environment Engineering, Adelaide Univ., Adelaide, SA 5005 Australia.

[2]Senior Lecturer, Dept. of Civil and Environment Engineering, Univ. of Melbourne, Parkville, VIC 3010 Australia. E-mail: n.lam@civag.unimelb.edu.au

[3]Associate Professor, Dept. of Civil and Environmental Engineering, Univ. of Melbourne, Parkville, VIC 3010 Australia.

[4]Project Manager (Civil), Mighty River Power, Ltd., P.O. Box 445, Hamilton, New Zealand.

Note. Associate Editor: Sashi K. Kunnath. Discussion open until August 1, 2004. Separate discussions must be submitted for individual papers. To extend the closing date by one month, a written request must be filed with the ASCE Managing Editor. The manuscript for this paper was submitted for review and possible publication on October 2, 2001; approved on September 16, 2003. This paper is part of the ***Journal of Structural Engineering***, Vol. 130, No. 3, March 1, 2004. ©ASCE, ISSN 0733-9445/2004/3-423–432/$18.00.

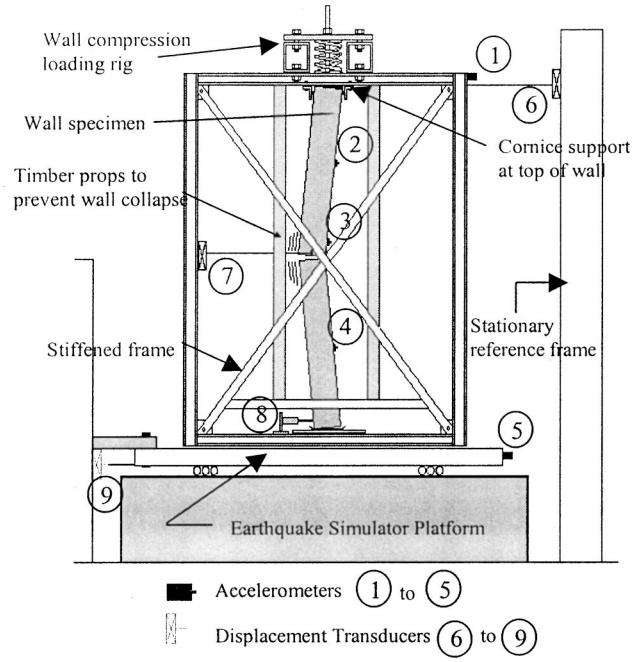

Fig. 1. Test rig configuration

control the seismic response of URM walls. Importantly, the construction of a suitable substitute structure for an URM wall and the comparison of seismic demand with wall displacement capacity are included to illustrate its application in a displacement-based design procedure.

Description of Experimental Tests

Experimental Test Setup

A total of 14 one-way vertically spanning URM wall panels were constructed for out-of-plane static and dynamic testing. The 1.5-m-tall test specimens had a wall thickness of either 110 or 50 mm, corresponding to wall slenderness ratios (h/t) of 13.6 and 30, respectively. A professional bricklayer was employed to construct the test specimens using clay bricks and a typical Australian mortar mix of 1:1:6 (cement:lime:sand) by volume. Each wall panel was constructed on a 100-mm-thick concrete slab with an embossed polythene membrane DPC connection located at the base of each wall. After curing for a minimum of 28 days, the walls were positioned on the department's shake table and prepared for testing, as shown in Fig. 1.

Test Rig

To simulate realistic boundary conditions at the top of each of the simply supported URM wall panels, a braced (stiff) steel frame was fixed to the shake table. The frame was used to provide lateral support for the top of each test specimen and in so doing imposed displacements to the top of the wall that were essentially the same as those at its base (refer to Fig. 1). This corresponds to situations in practice where the structure has a ''stiff'' horizontal floor diaphragm and the walls are well connected to the floor. The case of differential support motion, such as might occur in buildings with ''flexible'' floor diaphragms (Tena-Colunga and Abrams 1996), is also important but beyond the scope of this paper.

Table 1. Unreinforced Masonry Wall Material Properties—Test Results

Property	Mean	Standard deviation
Flexural strength, f_{mt}	0.49 MPa	0.15 MPa
Compressive strength, f_{mc}	13.4 MPa	1.64 MPa
Elastic modulus, E_m	9,400 MPa	5,322 MPa

Two boundary conditions were modeled during the tests: (1) ''cornice'' supports typically used to provide lateral restraint to the top of non-load-bearing walls and (2) slab supports to represent the case of a load-bearing wall. The cornice support (refer to Fig. 1) was made up of steel angle and 10 mm square, stiff rubber spacers to prevent the wall from binding against the angle at large wall midheight displacements. Prior to testing, the cornice was fitted snugly to the wall.

In order to simulate gravity loads on load-bearing walls, a vertical precompression force was applied at the top of the test walls. This was accomplished using six large springs to develop the required level of precompression stress, σ_v (refer to Fig. 1). The main difficulty in using this approach was that as the wall's midheight displacement increased, the top of the wall height was raised slightly, thereby increasing the spring precompression force. For example, the mean precompression force varied by less than $\pm 5\%$ for the 50-mm-thick wall specimens. However, the 110-mm-thick wall specimens suffered significant increases in precompression force at large displacements. For the 110-mm-thick walls, the constant force assumption was considered to be acceptable only for midheight displacements of less than 20% of the wall thickness. Thus, during tests with vertical precompression loading where out-of-plane rocking was allowed to take place, the maximum displacements were kept within this 20% limit.

Instrumentation

Nine channels of data consisting of horizontal accelerations (five channels) and displacements (four channels) were recorded for each of the dynamic tests in order to capture the dynamic response characteristics of the rocking URM wall specimens. As indicated in Fig. 1, accelerometers (channels 1–5) were positioned to record the horizontal accelerations of the shaking table, the top of the steel frame support, and at three (quarter) points along the height of the wall in order to capture the distribution of inertia forces acting on the wall. Horizontal displacements (channels 6–9) were recorded for the shake table, the top of the steel support frame, the wall midheight, and at its base relative to the shake table. This enabled direct calculations to be made of the wall deformation relative to its supports. During static tests, a load cell was used to record the applied force in addition to the wall displacements.

Material Properties

The key material properties typically used for design were measured using standardized tests such as bond wrench and compression tests of brickwork prisms and mortar cubes. The results of these tests (refer to Table 1), wall flexural strength of 0.49 MPa, and elastic modulus of $\sim$8–9 GPa, indicate that the test panels were representative of good quality masonry.

Table 2. Result Summary of Static Push Tests

Wall state	Vertical precompression σ_V (MPa)	Predicted strength (kN)		Experimental results (mean values)	
		LE theory	RB theory	F_{max} (kN)	Δ_W at F_{max} (mm)
Uncracked 110 mm walls	0	2.64	0.41	2.79	0.46
	0.15	4.82	5.31	5.75	21.2
Uncracked 50 mm walls	0.075	1.07	0.59	0.95	0.79
Cracked 110 mm walls	0	0.27	0.41	0.34	10.2
	0.15	2.32	5.31	4.36	18.5
Cracked 50 mm walls	0	0.07	0.11	0.083	8.3
	0.075	0.29	0.59	0.49	8.3
	0.15	0.47	1.07	0.71	10

Note: LE theory=linear elastic analysis, top and bottom reactions at centerline, $f_{mt} \neq 0$; RB theory=rigid body analysis, top and bottom reactions at leeward face of wall, $f_{mt}=0$.

Experimental Test Program

The experimental program was divided into three phases, namely: (i) testing for the nonlinear force–displacement behavior; (ii) testing for dynamic characteristics (i.e., natural frequency and damping); and (iii) testing for response to earthquake-induced support motions.

In the first phase of testing, static push-over and confirmatory dynamic tests (using harmonic support excitations) were used to investigate the nonlinear force–displacement ($F-\Delta_W$) behavior of simply supported URM walls. Loading was applied for the static tests at the wall midheight using a hand pump driven hydraulic actuator operated under displacement control. The braced steel support frame was used to simply support the wall panels at their top in these tests. Static tests were conducted on both ''uncracked'' and ''precracked'' wall test specimens. Harmonic support excitation tests (at frequencies of 2, 7, or 10 Hz) were conducted to compare static and dynamic strength and stiffness.

In the second phase of testing, the basic dynamic characteristics (natural frequency and damping) of the URM walls were studied using devices that set the wall into free vibration. These tests served to highlight significant displacement-dependent behavior. The free-vibration tests were performed on walls in their uncracked condition using a rubber mallet to apply a small impulse force at their midheight. Free-vibration tests on walls that were precracked (due to prior tests) involved displacing the walls at their midheight, releasing them from this initial position, and allowing them to vibrate freely until stopping in their vertical ''at-rest'' position.

In the final phase of testing, wall specimens were subjected to true inertial loading. Two types of dynamic support motion were employed in this phase of the experimental program. These were:

1. Impulse support displacements over a range of frequency (0.5–3.0 Hz) and amplitude; and
2. Four different earthquake excitations covering a range of intensity and frequency characteristics.

A summary of the test results is given in the following sections, followed by a detailed discussion of the results.

Test Results

Static Tests

A summary of the key experimental results for the static push tests and a comparison with analytical predictions is given in Table 2. The experimental values for maximum applied load, F_{max}, and wall midheight displacement, Δ_W, when the maximum force was recorded, are given in columns 5 and 6, respectively. Several general observations can be made. First, the uncracked wall strengths were greater than the precracked wall strengths (for the same value of vertical precompression load σ_V). Second, predictions of the force to cause cracking using quasistatic ''linear elastic'' (LE) theory [column 3] compare well with the experimental values [column 5] for the uncracked walls. The LE strength, assuming that the wall was uncracked and the top and bottom wall reactions remained at the wall centerline, is given by

$$F_{LE}=\frac{4}{h}Z(f_{mt}+f_d) \tag{1}$$

where Z=section modulus for the wall cross section; h=wall height; and f_d=compressive stress at the wall's midheight due to the vertical load applied at its top (σ_V) plus the weight of the upper half of the wall ($W/2$). The average experimental flexural tensile bond strength value, f_{mt}, of 0.49 MPa was used in the LE calculations.

Third, predictions using ''rigid body'' (RB) theory [column 4], as described by Doherty (2000), compare reasonably well with test results [column 5] for the precracked walls. The RB strength, corresponding to calculations with the top and bottom wall reactions located at the leeward face of the wall (i.e., side opposite to loading side), and assuming that the wall was precracked at its midheight, i.e., $f_{mt}=0$ in the midheight bedjoint, are given by

$$F_{RB}=\frac{3t}{h}W(1+\psi) \tag{2}$$

where W and h=as above; t=wall thickness; and ψ=ratio of the applied vertical load to the weight of the upper half of the wall.

A representative selection of the experimental force versus midheight displacement plots is presented in Fig. 2 for 50- and 110-mm-thick walls. Each wall was tested first in its uncracked state and then retested in its precracked condition. The RB analysis curves are also shown in Fig. 2.

Fig. 2(a) shows a typical load–deflection curve for a 110-mm-thick wall ($h/t=13.6$) with $\sigma_V=0$. In the initial phase of loading, the wall response is essentially linear for both cases. The uncracked wall response remained linear until the wall cracked at a force level that is closely predicted by LE theory. At this point the force quickly drops off and approaches the force predicted by RB

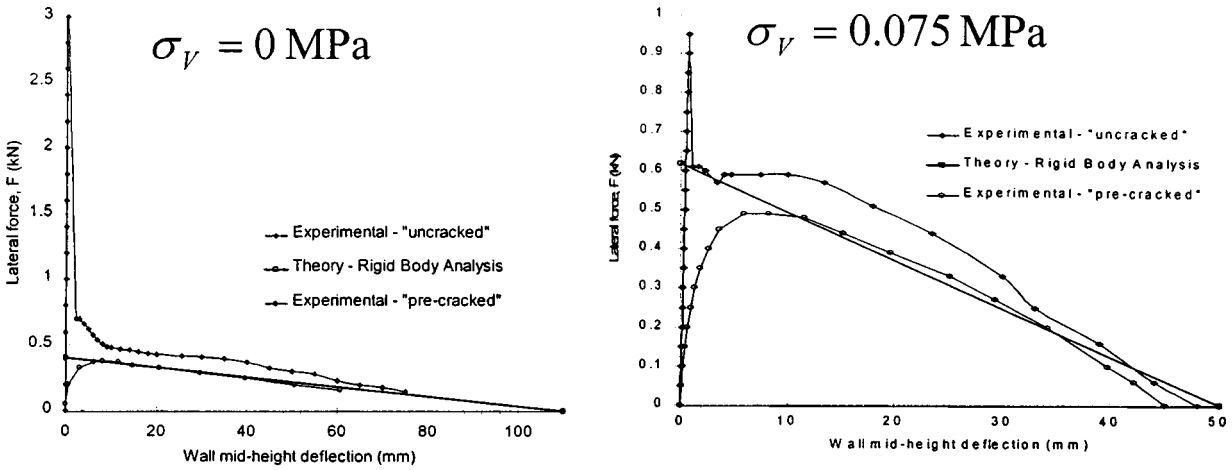

Fig. 2. Static test results

theory. The precracked wall response is also initially linear but becomes highly nonlinear as it approaches the cracking displacement, $\Delta_{CR} \approx 1$ mm. From this point on, the curve approaches and is well approximated by the RB theory curve.

Fig. 2(b) shows the results for a 50-mm-thick ($h/t = 30$) wall with a vertical precompression stress $\sigma_V = 0.075$ MPa. The general trends are similar although in the presence of vertical precompression the difference in magnitude of the uncracked and precracked strengths is less.

From these tests it was found that walls with $\sigma_V = 0$ generally cracked at displacements of less than 1 mm, or 0.1% drift. Importantly, the area under the linear elastic segment of the uncracked load–deflection curve is comparatively small compared to the total area under the load–deflection diagram. This implies that the elastic strain energy that can be stored in a wall prior to cracking is relatively small and quite possibly insufficient to instigate an ''explosive'' wall failure under dynamic loading.

Harmonic Excitation Tests

To examine the dynamic response characteristics for both uncracked and precracked walls, harmonic tests were conducted on walls in each state. In these tests a 2, 5, 7, or 10 Hz harmonic excitation, gradually increasing in amplitude, was used to drive the shake table. It was observed in the harmonic tests that the uncracked walls did not fail immediately after cracking in the midheight bedjoint. Instead, the wall response reached a steady-state response (instead of instability), rocking as a pair of rigid bodies. It was concluded that for most practical cases, nonlinear cracked behavior is more relevant to a dynamic scenario than a wall's elastic uncracked properties. Consequently, displacement rather than acceleration (force) was the critical parameter that determined wall stability irrespective of the initial state of the wall. Detailed descriptions of the full set of test observations can be found in Doherty (2000).

Fig. 3 presents a comparison of the static versus dynamic $F-\Delta_W$ characteristics for the 50-mm-thick ($h/t = 30$) walls. The dynamic force values are based on maximum acceleration and displacement values from a given cycle of response during harmonic tests. The comparisons are made for three levels of vertical precompression. From these data it was concluded that static test data provide a good approximation of dynamic response. This implies that simple force–displacement relationships can be used to develop reasonably accurate dynamic models. Importantly, the data also support the notion that displacement is the crucial response parameter. Failure occurs only when $\Delta_W > \Delta_f$.

Free-Vibration Tests

In order to investigate the natural frequency of vibration and damping levels for the simply supported uncracked wall specimens, a force pulse was applied to the wall midheight using a rubber mallet. Standard calculations from the time history response indicated that the natural frequency of vibration was approximately 19 Hz for an uncracked non-load-bearing 50-mm-thick wall and 42 Hz for an uncracked 110-mm-thick wall. The natural frequency was observed to be relatively constant over the exponential decay for the uncracked walls.

Free-vibration tests were also performed on test specimens that were precracked at their midheight. To undertake these tests, the midheight of a precracked (by prior testing) wall panel was displaced statically to near its point of instability displacement Δ_f. From this position, the wall specimens were released and permitted to rock freely. Energy losses associated with the inter-

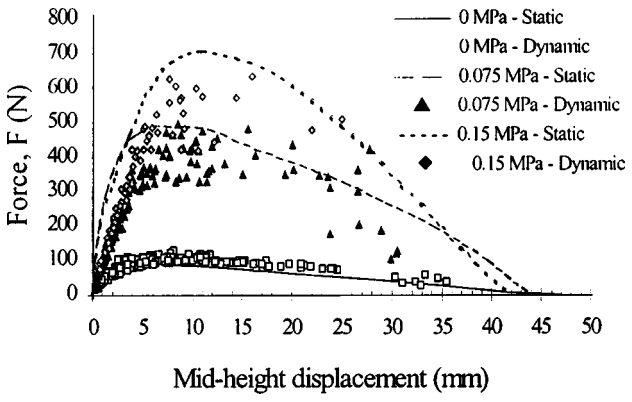

Fig. 3. Static versus dynamic test results

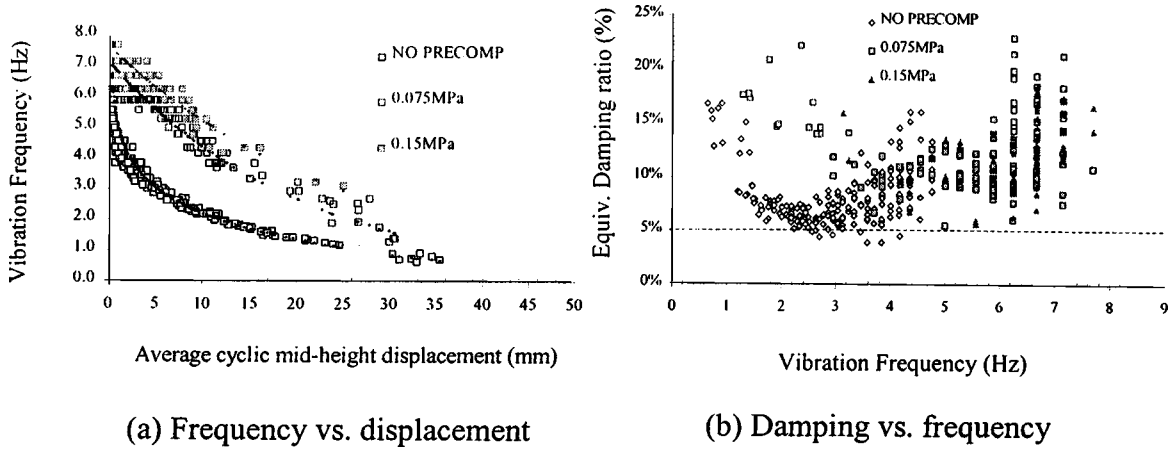

(a) Frequency vs. displacement (b) Damping vs. frequency

Fig. 4. Nonlinear frequency and damping relationships

nal damping, the cracks opening and closing, and friction at their supports were determined using the logarithmic decrement method.

From such data it was observed that frequency and damping are both displacement dependent for $\Delta_W > \Delta_{CR}$. The nonlinear relationship between frequency and displacement is illustrated in Fig. 4(a), where frequency is plotted versus displacement for the 50-mm-thick ($h/t=30$) walls for three different levels of vertical precompression ($\sigma_V=0$, 0.075, and 0.15 MPa). For any level of vertical load, the frequency of rocking reduces as the rocking displacement increases. At low levels of displacement, the rocking frequency approaches the uncracked natural frequency. Furthermore, the rocking frequency increases with vertical precompression. Equivalent viscous damping ζ_e values have been obtained for the wall specimens from the free-vibration experiments. Individual results obtained for each response half cycle are plotted as a function of the wall instantaneous rocking frequency [see Fig. 4(b)]. Limited resolution in the displacement measurement led to the scatter, which is most pronounced in the higher frequency range (when the displacement of the wall at the peak of the cycle is smaller). The observed equivalent viscous damping ratio ranged fairly widely, although a common lower bound of 5% was observed for both sets of walls ($h/t=13.6$ and 30). Thus, a Rayleigh damping model, which provides a lower-bound envelope to the results, could be used to define the frequency-dependent damping for the wall. Alternatively, a lower-bound ζ_e value of the order of 5% may be adopted in a linearized substitute-structure model, which assumes a constant value of ζ_e (Doherty et al. 2002).

Impulse Tests

The shaking table input selected for transient excitation tests included both impulse and real earthquake excitations. The range of amplitude and frequency content was selected to permit the rocking wall response to be thoroughly examined over a relevant range of excitation frequencies. This allowed critical excitation parameters to be identified and directly related to the wall response. The resulting dynamic data were also used to provide a basis for comparison with analytical response predictions using specially developed time–history analysis techniques (Doherty 2000).

As part of this test series, half-sine-wave and Gaussian impulse support motions were used to drive the shaking table with the test walls mounted on the shaking table, as shown previously in Fig. 1. Tests were performed on precracked simply supported URM walls with and without vertical precompression loads. The support displacement impulse frequencies used for the experimental investigation ranged from 0.5 to 3 Hz. This frequency range was selected to bracket the range of expected resonant rocking frequencies for the walls being tested. In each test, the impulse displacement amplitude input to the shaking table was

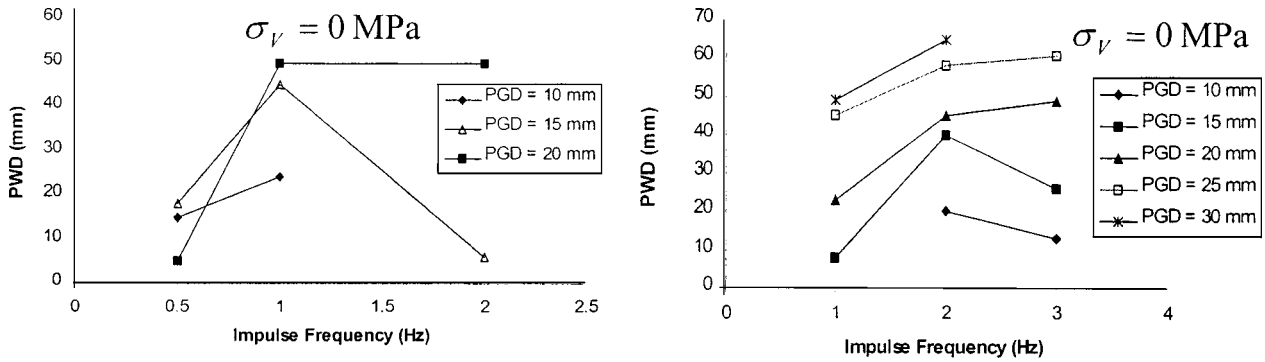

(a) 50 mm wall (b) 110 mm wall

Fig. 5. Impulse test results

Table 3. Summary of Key Earthquake Excitation Test Results (110 mm Walls) ($\sigma_V = 0$ MPa)

Excitation[a]	PGD (mm)	PWD (mm)	PGA (g)	PWA (g)
100% NH	4.2	9	0.23	0.26
200% NH	8.3	21	0.46	0.26
300% NH	12.5	28	0.69	0.26
400% NH	16.6	32.5	0.92	0.26
50% EL	81.5	44	0.18	0.27
66% EL	107.6	Failed	0.23	—
80% EL	130.4	Failed	0.28	—
100% EL	163.0	Failed	0.35	—
50% PD	27.0	41	0.22	0.34
66% PD	35.6	65	0.28	0.32
80% PD	43.1	87	0.34	0.34
100% PD	53.9	Failed	0.43	0.34

Note: PGD=peak ground displacement; PWD=peak wall displacement; PGA=peak ground acceleration; PWA=peak wall acceleration.

[a]NH=Nahanni; EL=El Centro; and PD=Pacoima Dam.

gradually increased at each frequency until rocking and ultimately instability of the wall occurred. The peak impulse displacement [peak ground displacement (PGD)] was related to the peak wall displacement (PWD) (at midheight) for each test specimen.

Fig. 5 plots the PWD versus frequency for 50- and 110-mm-thick walls over a range of impulse motion frequencies. Each curve, or ''contour,'' in Fig. 5 corresponds to a constant impulse displacement (PGD). On examination of the results it was evident that the maximum wall responses were associated with a specific frequency. This suggested that an ''effective resonant frequency'' existed for each wall (e.g., 1 Hz for the 50 mm wall and 2–3 Hz for the 110 mm wall), in spite of the highly nonlinear dependency of frequency on displacement shown previously in Fig. 4 for walls in the postcracking range of response. This is an important observation since displacement-based assessment methods use a substitute structure with a corresponding effective natural frequency.

Earthquake Tests

To complete the investigation into the response of both load-bearing and non-load-bearing simply supported URM walls to transient excitations, shaking table tests were performed using real earthquake accelerogram records to drive the shaking table. A comparison of response spectra for the actual table accelerations and the original accelerograms has shown a reasonable level of correlation in the frequency range of interest.

To investigate wall response over a range of excitation, relevant real earthquake scenarios of both ''low-frequency–large-displacement'' and ''high-frequency–small-displacement'' excitations were selected (Doherty et al. 2002). By comparing the PGD and peak ground acceleration (PGA) [refer to columns 2 and 4, Table 3], an indication of the type and severity of the earthquake can be attained. For instance, the 1985 Nahanni aftershock has a relatively high PGA (0.23 g) but a small PGD (4.2 mm) indicating that this earthquake had a dominant high-frequency component. Although traditionally this would not be expected to impact greatly on ductile structures, the large accelerations could be expected to more severely affect stiff brittle structures. The 1994

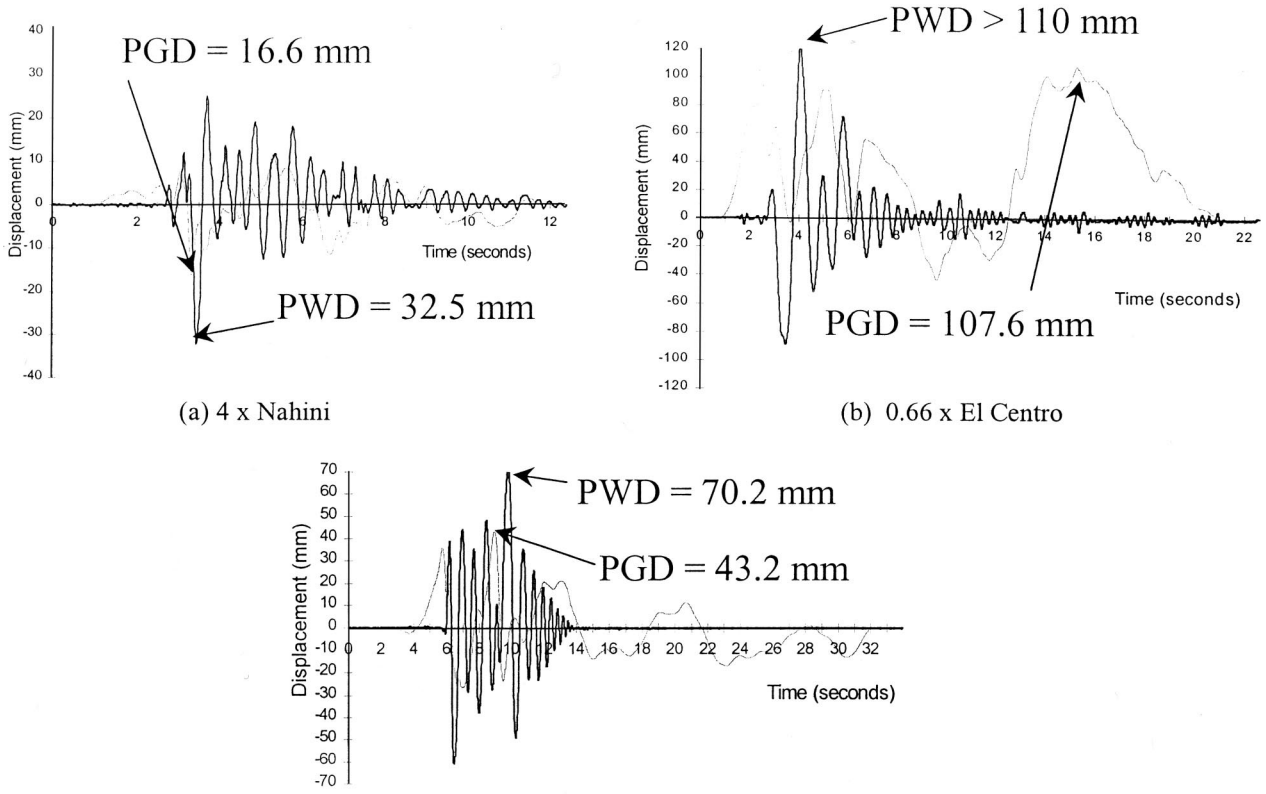

Fig. 6. Earthquake test results (110 mm wall) (PGD=peak ground displacement; PWD=peak wall displacement)

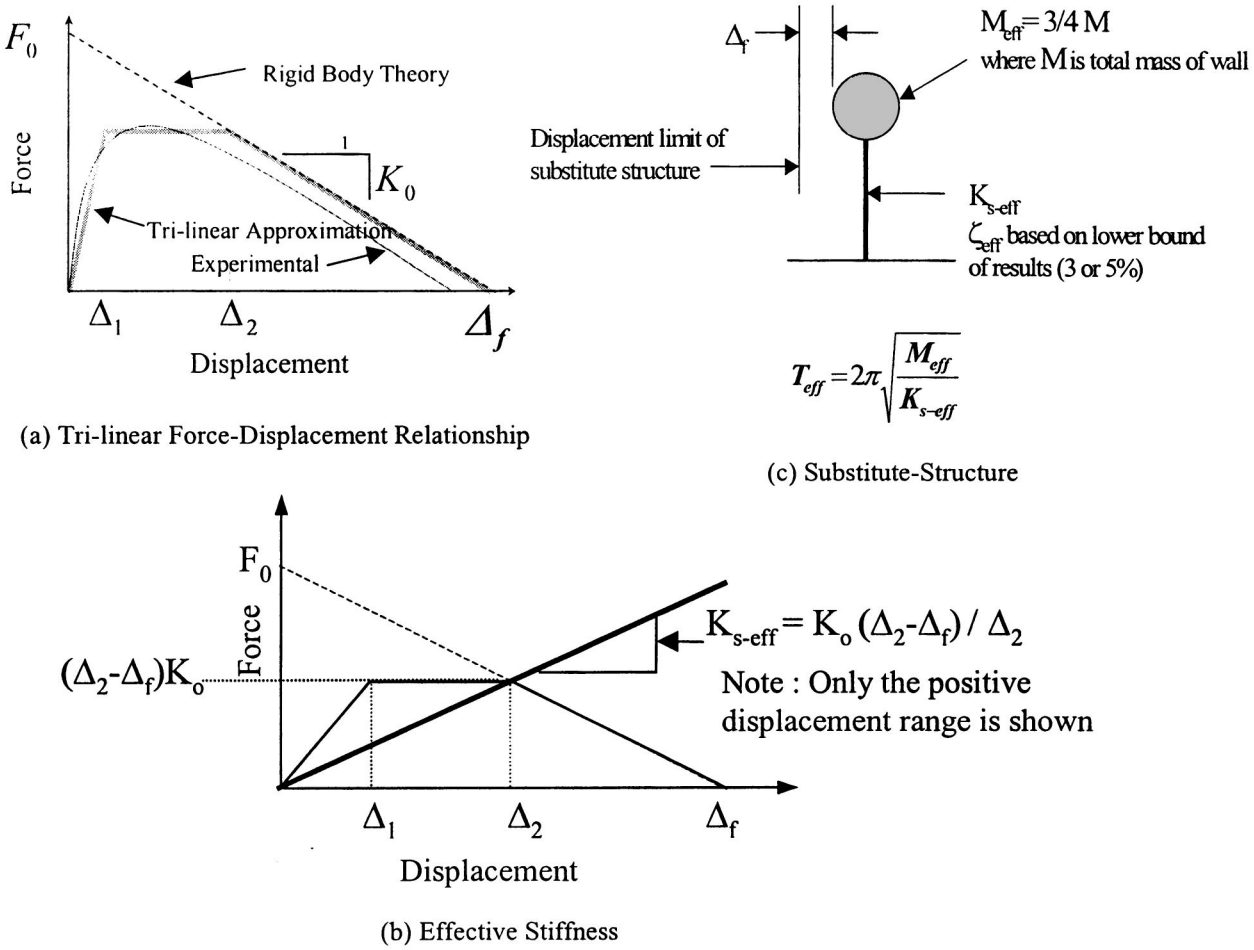

Fig. 7. From trilinear force–displacement model to substitute structure

Northridge (Pacoima Dam Site) and 1940 El Centro records typically have higher PGD and similarly large PGA, thus indicating lower dominant vibration frequencies.

In a similar fashion to the impulse tests, progressively increasing amplitudes of earthquake excitation (reported as percentages of the actual ground motion) were applied until rocking, and ultimately, instability of the wall specimen occurred. The peak ground (i.e., shaking table) displacement (PGD) and acceleration (PGA) were then related to the peak midheight wall displacement (PWD) and acceleration [peak wall acceleration (PWA)] for each test specimen.

A selection of test results is presented here (Fig. 6). The peak midheight wall displacement response (PWD) and input displacements (PGD) are compared. Table 3 presents a summary of the key results of the earthquake tests performed for the 110-mm-thick walls.

From Fig. 6(a) it can be seen that four times the Nahini earthquake, with its high PGA (0.92 g=4×0.23 g) was able to initiate rocking, but with its modest PGD (4×4.2 mm) was unable to cause failure. In contrast, 66% times the El Centro motion failed the 110 mm wall [Fig. 6(b)] even though its PGA (0.23 g =0.66×0.35 g) was much smaller than four times the Nahini PGA (0.92 g) since its PGD (108 mm=0.66×163 mm) was much greater than the PGD for 4×Nahanni (16.8 mm=4×4.2 mm). Similar results were observed for the 50-mm-thick walls.

Discussion of Test Results

In general, it was observed that failure always occurred once the PWD was greater than Δ_f. In contrast, walls did not always fail when the wall accelerations were greater than the acceleration capacity calculated using static force-based analysis methods. This result strongly suggested that a displacement-based design procedure would be more reliable in assessing the seismic capacity of URM walls subject to out-of-plane inertial loading. The major difficulty lies in how to accurately predict the PWD for a given earthquake motion with a specified PGA and PGD.

Data recorded during many quasistatic and dynamic tests of 14 simply supported walls confirmed that the dynamic $F-\Delta_W$ response can be accurately represented by the static response. This result, combined with the observation that displacements can be used to dictate whether wall failure occurred, led to the development of a displacement-based method for assessing the seismic capacity of URM walls. The method relies on a substitute structure (Shibata and Sozen 1976) with an effective secant stiffness and mass (and corresponding natural frequency and damping). A key step in this method of analysis is the specification of a nonlinear force versus displacement relationship suitable for use with a substitute structure. The trilinear relationship shown in Fig. 7(a) has been proposed by the authors (Doherty et al. 2002) for use in such an approach. The trilinear model is based on the results of

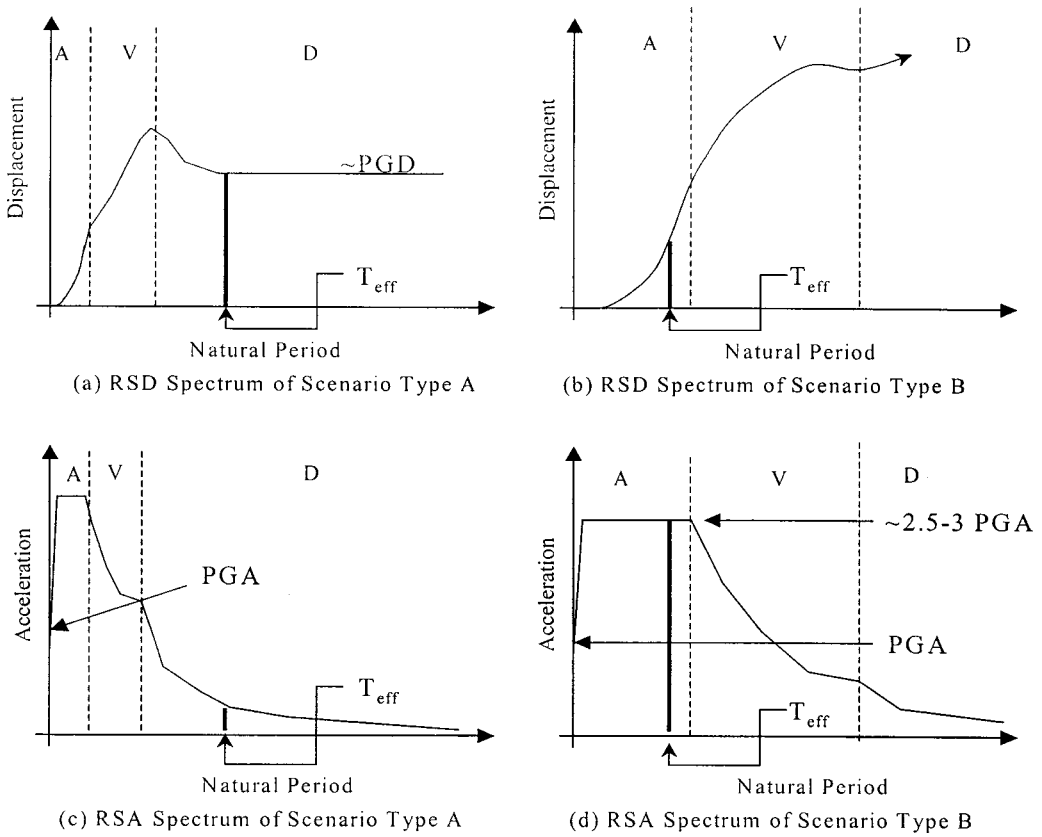

Fig. 8. Acceleration and displacement demands

the static and dynamic tests reported here. The trilinear model can be described in terms of the wall's RB strength, F_0; the softening slope, K_0, of the $F-\Delta_W$ curve given by RB theory; and the ratios of Δ_1/Δ_f and Δ_2/Δ_f, which depend upon the state of degradation in the mortar joints.

Throughout the series of harmonic tests on walls with $\sigma_V = 0$, the ability of mortar joints to sustain repeated loading cycles during rocking was found to be very good with only minor degradation observed. Results from static push tests were used to quantify the degradation of the mortar joints caused by dynamic testing. Full details of these tests are given in Doherty (2000) for walls in "new," "moderately degraded," and "severely degraded" conditions. The interpretation of the moderately and severely degraded conditions is highly subjective. However, observations of the degradation that occurred in the $F-\Delta_W$ response over many repeated tests of the walls have enabled the authors to quantify these parameters for three levels of wall degradation (Doherty et al. 2002). From the experimental tests, the effective width of the mortar in the cracked bedjoint for walls classified as severely degraded was approximately 90% of the original width. Moderately degraded walls had effective bedjoint widths that were essentially equal to their original widths. However, the exposed vertical faces of the mortar joints had rounded due to some rocking having taken place.

The trilinear model, so established from the presented test results [Fig. 7(a)], can be linked to the wall effective (or secant) stiffness [Fig. 7(b)], which can in turn be used to construct a substitute structure for the wall, as shown in Fig. 7(c). Full explanations for the equations annotated in Figs. 7(a) and 7(b) have been provided by Doherty et al. (2002). The linearization enables the wall ultimate displacement limit (Δ_f) to be compared conveniently with the displacement demand, which is defined by the displacement response spectrum [see Figs. 8(a) and 8(b)].

The results obtained from shaking-table simulations of real earthquake records (e.g., Fig. 6) show significant variations in the way the wall response behavior is related to the earthquake motion properties. This phenomenon is explained in the following by referring to two extremely different earthquake scenarios: (A) a small magnitude earthquake which generates high frequency motion on a rock or stiff soil site at close range [Figs. 8(a) and 8(c)] and (B) a large magnitude earthquake generating motions that possess a broad range of frequencies characteristics [Figs. 8(b) and 8(d)]. The acceleration and displacement response spectra (RSA and RSD) associated with the two earthquake scenarios are presented schematically in Fig. 8. Full explanations for the spectral form and the relationship between RSA and RSD for both rock and soil sites are provided by Lam (2000, 2001). The symbols "A," "V," and "D" denote the constant acceleration, velocity, and displacement regions, respectively. The wall response behavior in the two scenarios can be very different, even though failure is always defined at the point where the displacement demand exceeds the wall displacement capacity. Behavior in the type A scenario is clearly controlled by displacement [or by PGD, as shown in Fig. 8(a)]. This applies to cases where the wall effective period is high (due to high aspect ratio and low precompression) in comparison with the dominant period of the applied excitation. In contrast, the type B scenario characterized by high period motions, low aspect ratio, and/or high precompression, shows an acceleration controlled behavior [Fig. 8(d)].

Importantly, the force (acceleration) and the displacement approach could be made to provide similar predictions for the wall response behavior. Interestingly, a wall can be deemed safe by an

assessment based on either of the approaches. For example, the wall cannot overturn in either scenario if the highest point of the RSD spectrum is within the ultimate displacement limit of the wall. However, this peak displacement demand seems easier to ascertain in scenario A than scenario B. In low and moderate seismic regions characterized by small magnitude (''bulls-eye'') earthquakes, the displacement demand is typically limited [Fig. 8(a)]. In this context, displacement seems to be a more direct, and convenient, parameter to define seismic demand and capacity.

Closing Remarks

The results of many static and dynamic tests on 14 unreinforced brick masonry walls can be summarized as:

- Static force–displacement relationship can be reasonably modeled by a trilinear relationship that can be defined in terms of F_0, K_0, Δ_1/Δ_f, and Δ_2/Δ_f, which define the initial elastic stiffness, a maximum force plateau, and the slope of the backbone curve (which can be accurately defined from semirigid body theory of a wall rocking about its cracked sections). For the vertically spanning walls considered in this research, cracks formed at the base and top of wall supports and in a bedjoint at the wall midheight.
- Values for the ratios of Δ_1/Δ_f and Δ_2/Δ_f are dependent on the condition of the mortar joints.
- The dynamic hysteretic curve is accurately bounded by the static force–displacement relationship.
- Walls whose ''cracking,'' or ultimate, strength was reached during harmonic excitation tests did not collapse, even when subjected to support accelerations well in excess of their cracking limit. This confirmed that the ultimate behavior of the walls is governed not simply by acceleration (force).
- Free-vibration tests confirmed that wall rocking frequency and damping is displacement dependent. A lower bound of 5% damping was observed in these tests.
- Results of support impulse excitation tests indicate that the wall response is frequency sensitive, suggesting that they have a particular bias for an ''effective'' natural frequency where displacement amplification is greatest. This suggests that the dynamic response of a rocking URM wall can be approximated by a linearized displacement-based procedure.
- Earthquake excitation tests confirmed that displacements, rather than accelerations, dictate whether a wall collapses.

Acknowledgments

This research was conducted with the financial support of Australian Research Council Grant No. A89702060. The views expressed are those of the writers and not necessarily those of the sponsor. The writers would also like to acknowledge the technical assistance of Bruce Lucas, Greg Atkins, David Hale, and Geoffrey Hiorns in undertaking this experimental research.

Notation

The following symbols are used in this paper:

E_m = Young's modulus of elasticity for the brickwork (MPa);
F = horizontal force applied to wall at its midheight (kN);
F_0 = the maximum wall strength according to RB theory (kN);
f_d = compressive stress on the midheight of URM wall;
f_{mc} = compressive strength of the brickwork (MPa);
f_{mt} = flexural tensile strength of the brickwork (MPa);
h = wall height (mm);
K_0 = slope of the RB analysis curve (kN/mm);
PGA = maximum ground/shake table acceleration (g);
PGD = maximum ground/shake table displacement = maximum of Δ_G (mm);
PWD = maximum horizontal wall displacement=maximum of Δ_W (mm);
t = wall thickness (mm);
Δ_{CR} = cracking displacement–horizontal wall displacement at which point wall cracks (mm);
Δ_f = failure displacement–horizontal wall displacement at which point wall becomes unstable (mm);
Δ_G = horizontal displacement of shaking table and base of wall (mm);
Δ_W = horizontal displacement of wall at its midheight (mm);
Δ_1 = empirical displacement at which wall's force–displacement relation reaches its maximum strength (mm);
Δ_2 = empirical displacement at which wall's maximum force plateau intersects with the RB analysis curve (mm); and
σ_V = vertical precompression load on brick walls (MPa).

References

Abrams, D. P., Angel, R., and Uzarski, J. (1996). ''Out-of-plane strength of unreinforced masonry infill panels.'' *Earthquake Spectra,* 12(4), 825–844.

Bariola, J., Ginocchio, J. F., and Quinn, D. (1990). ''Out-of-plane seismic response of brick walls.'' *Proc., 5th North American Masonry Conf.*, Univ. of Illinois at Urbana–Champaign, Urbana, Ill., June 3–6, 429–439.

Calvi, G. M., and Kingsley, G. R. (1995). ''Displacement-based seismic design of multi-degree-of-freedom bridge structures.'' *Earthquake Eng. Struct. Dyn.*, 24(9), 1247–1266.

Doherty, K. (2000). ''An investigation of the weak links in the seismic load path of unreinforced masonry buildings.'' PhD thesis, Dept. of Civil and Environmental Eng., Adelaide Univ., Adelaide, Australia.

Doherty, K., Griffith, M. C., Lam, N. T. K., and Wilson, J. L. (2002). ''Displacement-based seismic analysis for out-of-plane bending of unreinforced masonry walls.'' *Earthquake Eng. Struct. Dyn.,* 31(4), 833–850.

Ewing, R. D., and Kariotis, J. C. (1981). ''Methodology for the mitigation of seismic hazards in existing unreinforced masonry buildings: Wall testing, out of plane.'' *ABK Topical Rep. No. 04,* El Segundo, Calif.

Lam, N., Wilson, J., and Hutchinson, G. (1995). ''The seismic resistance of unreinforced masonry cantilever walls in low seismicity areas.'' *Bull. New Zealand Natl. Soc. Earthquake Eng.,* 28(3), 79–195.

Lam, N. T. K., Wilson, J. L., and Chandler, A. M. (2001). ''Seismic displacement response spectrum estimated from the frame analogy soil amplification model.'' *J. Eng. Struct.*, 23, 1437–1452.

Lam, N. T. K., Wilson, J. L., Chandler, A. M., and Hutchinson, G. L. (2000). ''Response spectrum modeling for rock sites in low and moderate seismicity regions combining velocity, displacement, and acceleration predictions.'' *Earthquake Eng. Struct. Dyn.,* 29(10), 1491–1526.

La Mendola, L., Papia, M., and Zingone, G. (1995). ''Stability of masonry walls subjected to seismic transverse forces.'' *J. Struct. Eng.*, 121(11), 1581–1587.

Magenes, G., and Calvi, G. M. (1997). ''In-plane seismic response of brick masonry walls.'' *Earthquake Eng. Struct. Dyn.*, 26(11), 1091–1112.

Moehle, J. P. (1996). ''Displacement based seismic design criteria.'' *Proc., 11th World Conf. on Earthquake Eng.*, Pergamon, Elsevier Science, Ltd., New York, *Disk 4, Paper No. 2125*.

Priestley, M. J. N. (1985). ''Seismic behavior of unreinforced masonry walls.'' *Bull. New Zealand Natl. Soc. Earthquake Eng.*, 18(2), 191–205.

Priestley, M. J. N. (1997). ''Displacement-based seismic assessment of reinforced concrete buildings.'' *J. Earthquake Eng.*, 1(1), 157–192.

Shibata, A., and Sozen, M. A. (1976). ''Substitute-structure method for seismic design in R/C.'' *J. Struct. Div. ASCE*, 102(1), 1–18.

Tena-Colunga, A., and Abrams, D. P. (1996). ''Seismic behavior of structures with flexible diaphragms.'' *J. Struct. Eng.*, 122(4), 439–445.